# Exploiting the surface geothermal energy to heat and cool buildings

Kheira Belhamideche[1], Nadia Laredj[1,2], Mustapha Maliki[1,2], Missoum Hanifi[1,2], Djihad Bennaceur[1], Mahi Eddine Brahimi[1]

[1] Laboratory of Construction, Transport and Environmental Protection LCTPE, University of Mostaganem-Algeria.
[2] Department of Civil Engineering, Faculty of Science and Technology, University of Mostaganem-Algeria
belhamideche1805@gmail.com

ABSTRACT: The thermal exploitation of the ground's surface layers is already common practice in many countries. Generally exploited using geothermal heat pumps to exchange and store heat from the ground. The efficiency of these systems is affected by many factors, among which climatic conditions and the thermal properties of the soil play a major role. The aim of this research work is to study the impact of different surface heat fluxes on the estimation of seasonal variations in ground temperature, and to determine the thermal energy close to the ground surface for use in heating and cooling buildings. A transient model based on the finite volume method "Comsol multiphysics", taking into account atmosphere-soil-heat exchanger interactions, is established for the resolution of the soil energy conservation equations and the soil surface water balance.
KEY WORDS: unsaturated soil, geothermal energy, convection, heat exchanger, atmospheric interaction

## 1 INTRODUCTION

The geothermal energy system is a renewable, durable and clean source for heating and cooling buildings, which is important for reducing building energy consumption and carbon emissions (Cheng et al. 2023). Geothermal heat pumps are extremely efficient for heating and cooling buildings. Of the various types of geothermal heat pump, horizontal ground heat exchangers (HGHE) are becoming increasingly popular due to their cost-effectiveness, ease of installation and high capacity for regeneration (Hu et al. 2023). However, these types of exchangers are more sensitive to atmospheric fluctuations and soil moisture dynamics, as they are buried at shallow depths (between 1.0 and 2.0 m)(Chalhoub et al. 2017)The neglecting soil moisture transfer or overstating soil saturation would overestimate the carrying capacity of the horizontal ground heat exchanger system (Gao et al. 2023). The spiral heat exchanger had the best thermal performance than the U-shaped and W-shaped heat exchangers in regard to both long-term and short-term thermal loads (Zhao et al. 2016).
In this context, a transient 3D numerical model basing on the finite element method to evaluate the performance of spiral horizontal heat exchanger placed 2 m below the ground surface was developed using the Comsol multiphysics software. The model takes into account the interaction between the soil atmosphere and the heat exchanger, and the transfer of water into the unsaturated soil.

## 2 THE PROPOSED NUMERICAL MODEL

In this work, the performance of horizontal geothermal heat exchangers is examined for a region located in north-west Algeria (Mostaganem). In this regard, a numerical model based on the finite element method was established using the multiphysics software Comsol taking into account the atmosphere-soil interaction, to simulate the effectiveness of a geothermal heat pump system in

combination with spiral horizontal ground heat exchangers. The proposed model includes moisture transfer in unsaturated soils, thermal and hydraulic properties of unsaturated soils, heat transfer in unsaturated soils and heat transfer in pipes.
The geometry of the study presents a 3D domain with a clayey soil, has a length of 20 m, a width of 15 m and a height of 10 m, the heat exchangers are comprised of high-density polyethylene (HDPE) pipes, the carrier fluid used in this study is water. The internal and external diameters of the exchanger are 0.02 m and 0.026 m respectively. The meshes created in this simulation are denser. A free tetrahedral mesh was used in the horizontal heat exchangers and in the surrounding soil. The total number of elements is 2448 with a minimum quality of 0,2. Figure 1 shows the geometry and mesh of the present study.

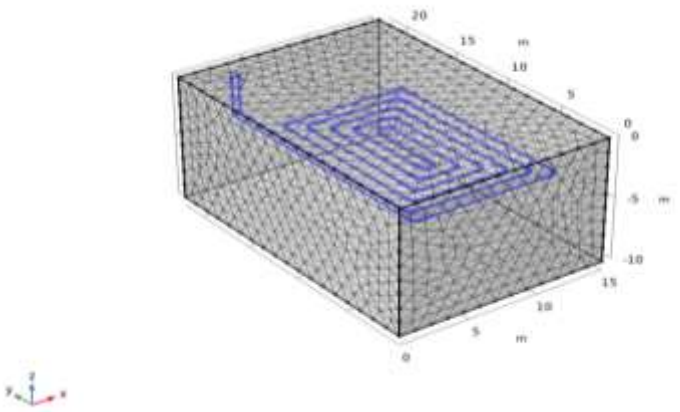


Figure 1. Domain geometry and mesh of numerical simulations

## 2.1 *The basic equations*

### 2.1.1 *Water transfer equation for unsaturated soils*

Richards' equation is used to calculate hydraulic variation with space and time (Tang and Nowamooz 2020).

$$\rho_w.\psi.\frac{\partial H_p}{\partial t} + \nabla.[-K.k_r.\nabla.\rho_w.(H_p + D + H_k)] = 0 \quad (1)$$

$\rho_w$ is the water density, $\psi$ is the specific moisture capacity ($m^{-1}$), $H_p$is the suction head (m), $K$ is the hydraulic conductivity ($ms^{-1}$), $k_r$ is the relative hydraulic conductivity, $D$ is the elevation head (m), $H_k$ is the kinetic head (m).

### *2.1.2 Soil hydraulic properties*

For hydraulic conductivity curves, we have:

$$K(H_p) = K_s K_r(H_p) = K_s(\alpha/(\alpha + |H_p|^{\gamma}) \quad (2)$$

$K_s$ is the saturated hydraulic conductivity, $\alpha$ and $\gamma$ are coefficients that depend on the dry density of the soil.
For water retention curves, we have:

$$\theta(H_p) = \theta_1(\alpha'/(\alpha' + |H_p|^{\beta}) + \theta_2 \quad (3)$$

$\theta_1$saturated volumetric water content, $\theta_2$ undrained volumetric water content, $\alpha'$and $\beta'$ are coefficients that depend on the dry density of the soil.

### *2.1.3 Modeling of ground surface temperature*

Heat transfer in the soil is given by the following equation:

$$\rho_s C_{ps} \frac{\partial T_s}{\partial t} = \nabla.(k_s \nabla T_s) + \nabla(\rho_w C_{pw} u_w T_s) + Q_s \quad (4)$$

Where $\rho_s$ is the soil density, $C_{ps}$ is the soil heat capacity, $k_s$is the soil thermal conductivity, $T_s$ is the soil temperature, $\rho_w$ is the water density, $C_{pw}$ is the specific heat capacity of water, $u_w$ is the water velocity in the soil and $Q_s$ is the soil heat source.

*2.1.4 Soil thermal properties* (Reiffsteck et al.), (Abu-Hamdeh 2003)

$$\mathrm{k_s} = 0.1442 \times (0.9\log\theta - 0.2) \times 10^{0.6243.\rho_d} \quad (5)$$

$$C_{ps} = (C_s + \theta C_w)/(1+\theta) \quad (6)$$

$\theta$ is the water content, $\rho_d$ is the dry density, $C_{ps}$ is the specific heat, $C_w\ is$ specific heat capacity of water and $C_s$ is specific heat of dry soil particles.

*2.1.5 Heat transfer in pipes*

The following expression is used to predict the Fluid flow and heat transfer within the pipes.

$$A\rho_f C_{Pf} \frac{\partial T_f}{\partial t} + A\rho_F C_{Pf} u_f.\nabla T_f = \nabla.Ak_f \nabla T_f + f_D \frac{\rho_f A}{2d_h}|u_f|u_f^2 + Q_{wall} \quad (7)$$

Where A is the internal cross-section of the pipe , $\rho_f$is the density of the fluid, $C_{Pf}$ is the specific heat capacity of the fluid, $T_f$ is the temperature of the fluid, $u_f$ is the fluid flow velocity , $k_f$ is the fluid thermal conductivity, $f_D$ is the Darcy friction factor, $d_h$ is the hydraulic diameter and $Q_{wall}$ is the energy of the surrounding medium .

## 3 THE INITIAL AND BOUNDARY CONDITIONS

The initial temperature of the soil and the temperature of the fluid circulating in the pipes are the same in this study, fixed at 16°C.
Since the soil at shallow depths is more affected by climatic fluctuations, we have taken into consideration the interaction between the atmosphere and the soil surface as a boundary condition. This interaction is given by the energy balance at the soil surface. At the bottom of the domain, we imposed a temperature of 16°C.
The energy balance at the ground surface is given by the following equation (Tang and Nowamooz 2020).

$$\mathrm{G} = \mathrm{R_n} + \mathrm{H} + \mathrm{LE} \quad (8)$$

G is soil heat flux, $R_n$ is the net radiation, H is the sensible heat and LE is the latent heat.

### 3.1 *The net radiation*

Net radiation includes absorption and reflection of short-wave radiation, as well as outgoing and incoming long-wave radiation, expressed as follows(An et al. 2017).

$$R_n = (1-\alpha)R_s + L_e - L_o - (1-\varepsilon o)L_e \quad (9)$$

$\mathrm{R_s}$ is shortwave radiation ($\mathrm{W/m^2}$), $\boldsymbol{\alpha}$ is the Albedo of the ground surface, $\mathrm{L_e}$ is the long-wave radiation entering ($\mathrm{W/m^2}$), $\mathrm{L_o}$ is the long-wave outgoing radiation ($\mathrm{W/m^2}$) and $\varepsilon o$ is the emissivity of the surface.

### 3.2 *The sensible heat fluxes*

Sensible heat flow is the transfer of convective heat between the surface of the ground and the surrounding air (Costa-Filho et al. 2021).

$$H = \rho_a \times C_p(T_s - T_a)/r_a \quad (10)$$

$\rho$ is the density of air (kg/m3), $C_p$is the specific heat capacity of air (J/kg/K), Ta is the air temperature, $T_s$ is the soil temperature and $r_{ah}$ is the aerodynamic heat resistance (s/m).

### 3.3 *Latent heat flux*

Latent heat flux is the energy that is absorbed by water at the surface of the ground by evaporation or transpiration. The latent heat flux is calculated as the latent heat of vaporisation of water (L) multiplied by the actual evaporation (E). Actual evaporation can be derived using the formula below (Pereira 1998)

$$E = P.[1 + \left(\frac{E_p}{P}\right)^{-2}]^{-1/2} \quad (11)$$

Where P is the precipitation rate (mm/s), Ep is the evaporation potential (Kg/m$^2$/s).
The Penman-Monteith formula is used to calculate the evaporation potential

$$E_p = \frac{1}{L}[\frac{\Delta.R_n + \rho_a.\frac{C_{p-a}(e_s - e_a)}{r_a}}{\Delta + \gamma\left(1 + \frac{r_c}{r_a}\right)}] \quad (12)$$

$\Delta$ is the slope of the saturation vapour pressure curve (kPa/K), $e_s$ is the saturation vapour pressure (kPa), $e_a$ is the actual vapour pressure (kPa), $\gamma$ is the psychrometric constant (kPa/K), $r_c$ is the resistance of the plant canopy (s/m).

Table1.Parameters used in the model

| Parameter | Description | Value |
|---|---|---|
| $\alpha$ | Albedo of the ground surface | 0.2 [-] |
| $R_{Si}$ | Short wave radiation | Calculated |
| $L\uparrow$ and$L\downarrow$ | Outgoing and incoming long-wave radiation | Calculated |
| $\rho$ | The density of air | 1.25 [kg/m3] |
| $C_p$ | The specific heat capacity of air | 1003[J/kg/K] |
| $z_m$ | Height of wind measurements | 2 [m] |
| $z_h$ | Height of humidity measurement | 2 [m] |
| $k$ | Constant of von Karman | 0.41 [-] |
| $U_z$ | Velocity of wind at height z | 2.5[m/s] |
| L | The length of the HGHEs | 30 [m] |
| $C_{Pf}$ | Fluid thermal capacity | 4200[J/(kg.K)] |
| $u_f$ | Fluid velocity inside HGHEs | 0.4[m/s] |
| $k_f$ | Fluid thermal conductivity | 0.591[W/ (m.K)] |
| $D_i$ | Inner diameter of HGHEs | 0.02 [m] |

## 4 RESULTS AND DISCUSSION

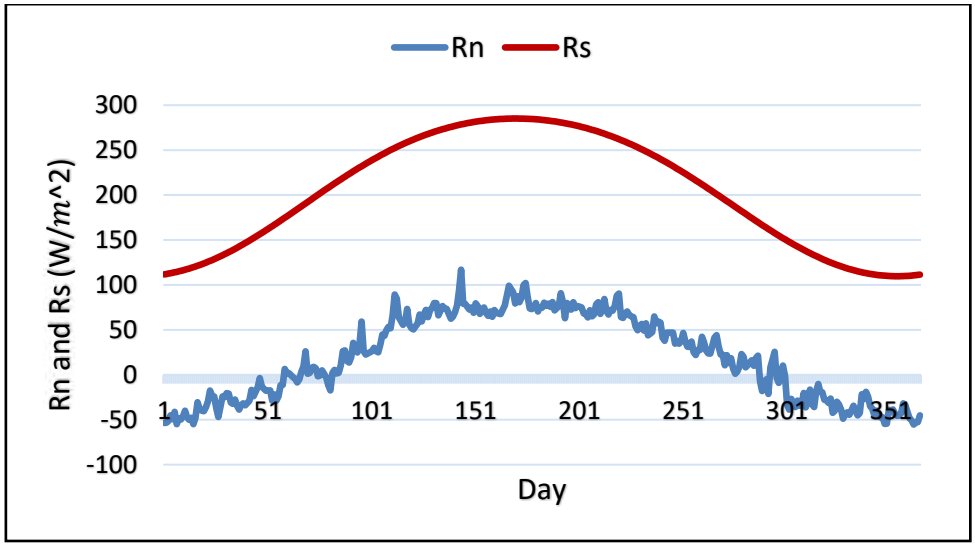


Figure 2. The net radiation and short-wave radiation in Mostaganem for the year 2022

Figure 2 shows the annual variation in net radiation Rn and short-wave radiation in Mostaganem for year 2022. The peak values for the 2 graphs are observed in summer (280 W/m$^2$ for Rs and 100 W/m$^2$ for Rn) because of the high insolation, the absence of clouds and the long daylight hours, as opposed to winter when the values are low (100 W/m$^2$ for Rs and -50 W/m$^2$ for Rn).

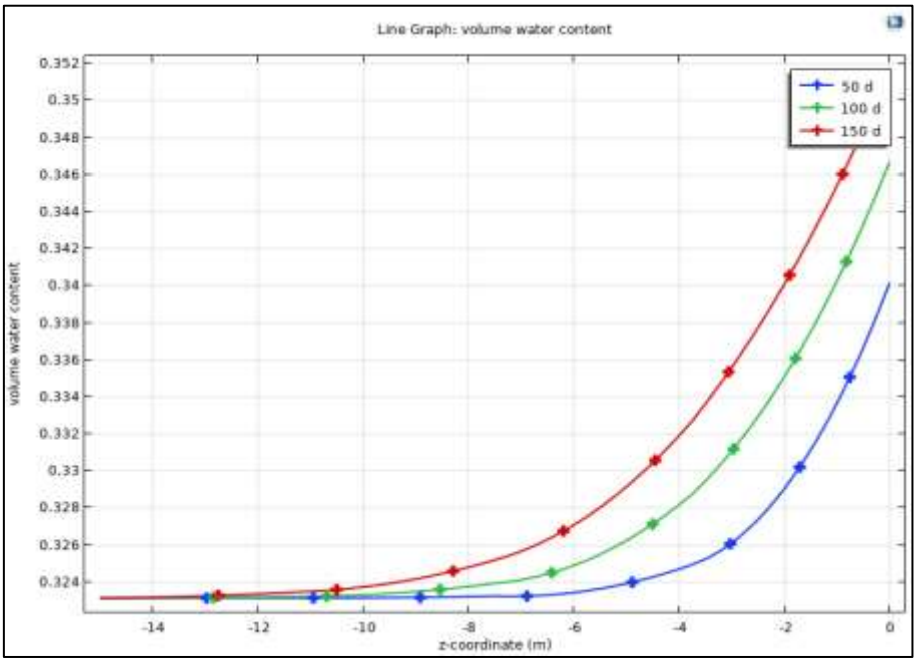


Figure 3. volumetric water content as a function of depth.

Figure 3 depicts the fluctuation of volumetric water content as a function of depth at t=50, 100 and 250 days in the year 2022.The results indicate that beyond 10 meters the volumetric water content is stable and permanent.

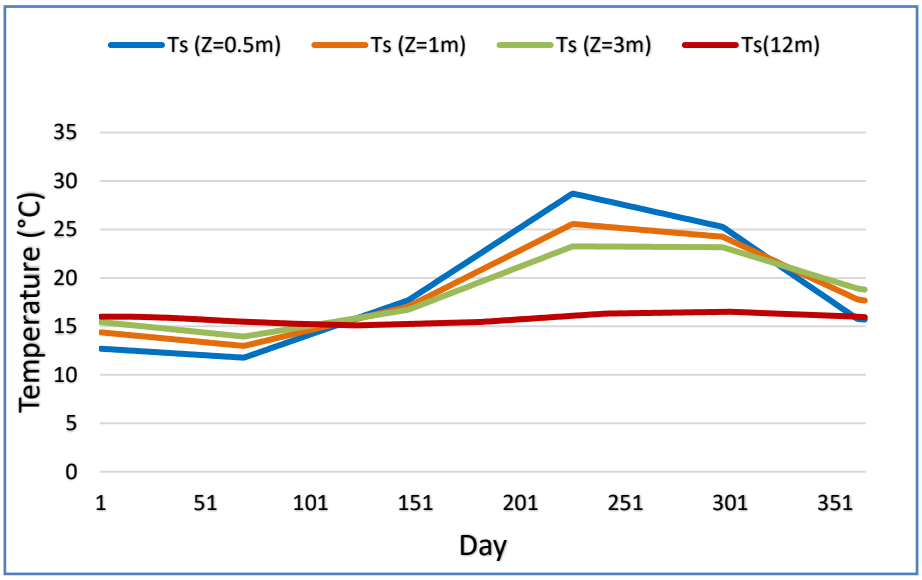


Figure 4. Ground temperature as a function of depth.

Figure 4 shows the evolution of soil temperature as a function of depth. it's clear that as soil depth increases, soil temperature fluctuation decreases until the soil reaches a depth of 10 meters, at which point soil temperature becomes constant.

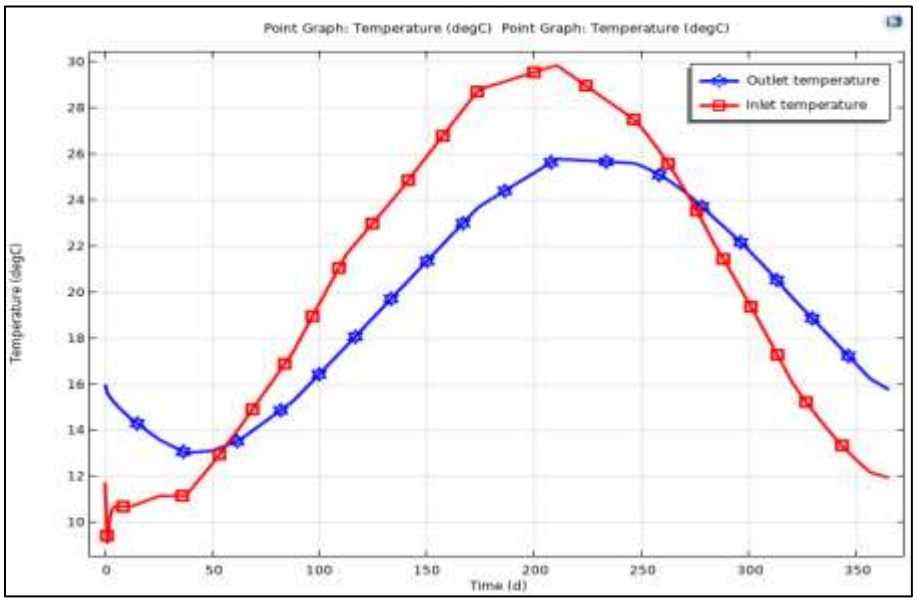


Figure 5. Fluid inlet and outlet temperatures for the year 2022

Figure 5 shows the fluid inlet and outlet temperature for the year 2022.The values of the fluid inlet temperature $T_{i,f}$ range between 10.24°C to 30°C, and the fluid outlet temperature $T_{0,f}$ range from 13.04°C to 25.8°C. There is a temperature difference of 4.2°C.

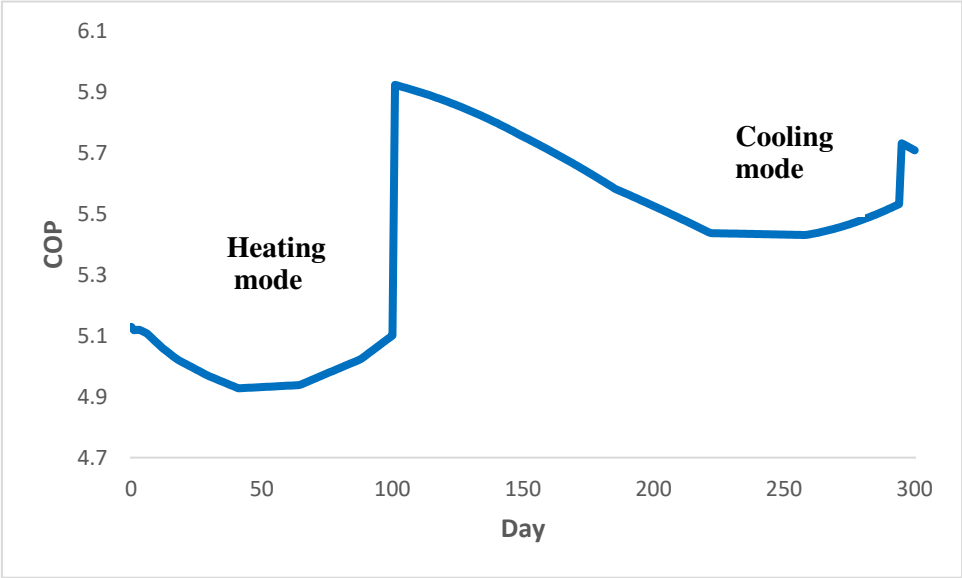


Figure 6. Performance coefficient in heating and cooling mode

Figure 6 shows the coefficient of performance of heat exchanger in heating and cooling mode. In heating mode, the coefficient is greater than 4,9. The highest value is 5,1.
In cooling mode, the performance coefficient is over 5,4. The highest value is 5,95.

## 5 CONCLUSION

A numerical model has been developed for the city of Mostaganem, taking into consideration the effects of all meteorological parameters (wind speed, ambient temperature, solar radiation, precipitation and sky temperature) and geological conditions.
Solar radiation has a significant influence on the temperature of the first few metres of soil, which is followed by sensible heat flux and latent heat flux in the case of the city of Mostaganem.
Ground temperature at shallow depths, up to 12 m below ground level, is influenced by daily and seasonal weather cycles. However, at depths greater than 12 m, the ground temperature remains relatively constant. This relatively constant temperature means that buildings can be heated and cooled over the long term.

## 6 PREFERENCES

Abu-Hamdeh NH (2003) Thermal properties of soils as affected by density and water content. Biosyst Eng 86:97–102. https://doi.org/10.1016/S1537-5110(03)00112-0

An N, Hemmati S, Cui YJ (2017) Assessment of the methods for determining net radiation at different time-scales of meteorological variables. Journal of Rock Mechanics and Geotechnical Engineering 9:239–246. https://doi.org/10.1016/j.jrmge.2016.10.004

Chalhoub M, Bernier M, Coquet Y, Philippe M (2017) A simple heat and moisture transfer model to predict ground temperature for shallow ground heat exchangers. Renew Energy 103:295–307. https://doi.org/10.1016/j.renene.2016.11.027

Cheng N, Zhou C, Luo Y, et al (2023) Thermal behavior and performance of shallow-deep-mixed borehole heat exchanger array for sustainable building cooling and heating. Energy Build 291:. https://doi.org/10.1016/j.enbuild.2023.113108

Costa-Filho E, Chávez JL, Zhang H, Andales AA (2021) An optimized surface aerodynamic temperature approach to estimate maize sensible heat flux and evapotranspiration. Agric For Meteorol 311:. https://doi.org/10.1016/j.agrformet.2021.108683

Gao W, Masum S, Qadrdan M, Rhys Thomas H (2023) A numerical study on performance efficiency of a low-temperature horizontal ground-source heat pump system. Energy Build 291:. https://doi.org/10.1016/j.enbuild.2023.113137

Hu L, Rizvi ZH, Tobber L, Wuttke F (2023) Thermal performance of three horizontal ground heat exchanger systems: comparison of linear-loop, spiral-coil and slinky-coil arrangements. Front Energy Res 11:. https://doi.org/10.3389/fenrg.2023.1188506

Pereira LS (1998) Crop evapotranspiration-Guidelines for computing crop water requirements-FAO Irrigation and drainage paper 56

Reiffsteck P, Couaillier M, Grandjean G VALIDATION D'UN SYSTÈME DE CLASSIFICATION THERMIQUE DES SOLS VALIDATION OF A THERMAL SOILS CLASSIFICATION SYSTEM

Tang F, Nowamooz H (2020) Outlet temperatures of a slinky-type Horizontal Ground Heat Exchanger with the atmosphere-soil interaction. Renew Energy 146:705–718. https://doi.org/10.1016/j.renene.2019.07.029

Zhao Q, Chen B, Liu F (2016) Study on the thermal performance of several types of energy pile ground heat exchangers: U-shaped, W-shaped and spiral-shaped. Energy Build 133:335–344. https://doi.org/10.1016/j.enbuild.2016.09.055

# INTERNATIONAL SOCIETY FOR SOIL MECHANICS AND GEOTECHNICAL ENGINEERING

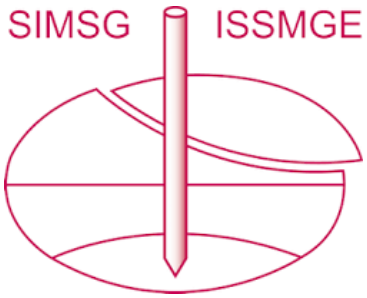


*This paper was downloaded from the Online Library of the International Society for Soil Mechanics and Geotechnical Engineering (ISSMGE). The library is available here:*

*https://www.issmge.org/publications/online-library*

*This is an open-access database that archives thousands of papers published under the Auspices of the ISSMGE and maintained by the Innovation and Development Committee of ISSMGE.*

*The paper was published in the proceedings of the 18th African Regional Conference on Soil Mechanics and Geotechnical Engineering and was edited by Abdelmalek Bekkouche. The conference was held from October 6th to October 9th 2024 in Algiers, Algeria.*